UNIVERSITY OF MINNESOTA

SOLAR VEHICLE PROJECT

MECHANICAL SYSTEMS STRUCTURAL REPORT

March 15, 2008

Project Advisors

Jeff Hammer
Patrick Starr

Mechanical Team Members

Jacob Hanna
Tristan Heller
Eric Heitman
Chris Hurley
Andrew Kirchman
Jason Loeffler
Sam Schibonski
Dave Hoffman
Taylor Hill

1 – Introduction/Overview

Since 1990, the University of Minnesota Solar Vehicle Project (UMNSVP) has produced seven world class race vehicles. New rules regarding the driver seating position added an additional challenge to the design of our solar vehicle, Centaurus.

The more upright driver seating position increases safety through improved visibility for the driver and increased crush space to the rear. In order to maintain the outstanding stability of the UMNSVP's previous cars, the position of the driver was lowered, which means that the center of gravity is approximately the same height as previous vehicles. Fiberglass, as opposed to carbon fiber, panels were used to increase fracture and conductivity resistance.

The decision to enter into the Stock Class was made primarily to maintain larger vehicle size for improved driver operating conditions and safety. This decision added to the challenges in designing the aerodynamics of the vehicle. While the the area of the car is large the coefficient of drag is low, resulting in similar aerodynamics to previous UMNSVP vehicles.

It is the intent of the this report to document the engineering decisions and features included in Centaurus. In addition, this report will demonstrate to NASC race officials that our entry is a safe, road worthy, and competitive vehicle. Any questions or concerns regarding the content of this report may be addressed to either our mechanical team leader or faculty advisors.

Jacob Hanna,
Mechanical Team Leader

Table of Contents

Introduction	**2**
Front Suspension	**4**
Rear Suspension	**6**
Chassis and Impact Analysis	**9**
Brakes	**20**
Steering	**22**
Appendix	**23**

2 - Front Suspension

2.1 Material Specifications

The front suspension utilizes a double a-arm system that is designed for low tire scrub and low weight. The lower a-arms are made from 0.750 [in] OD by 0.058[in] wall 4130 steel tubing. The upper a-arms are machined into a 0.5[in] x 0.5[in] section from 7075-T6 aluminum. The wheel hubs and uprights are CNC machined out of 7075-T6 aluminum. The axles are made from solid 0.669 [in] OD heat treated 4140 steel. The lower a-arms use 0.25[in] bore high misalignment rod end with 0.375 inch shanks. The upper a arms each have one .3125 [in] bore rod end with a .3125 inch shank, and one 0.25 inch rod end with a .375 inch shank. The lower a-arms are attached to the uprights by 0.375 [in] bore spherical bearings, and the upper a-arms are attached to the uprights with 0.25 [in] bore spherical bearings. The spherical bearings are mounted in machined cavities in the a arms and the arms are positioned so the legs are two-force members producing no bending moments. The bolts attaching the a arms to the upright utilize double shear mounting. The spring force from the shock absorber is directed toward the lower ball joint to reduce bending moments. The lower a-arm mounts to the chassis with two brackets machined out of 7075-T6 aluminum. These brackets are bolted to two perpendicular chassis panels. The upper a-arms attach to the chassis with 0.125 [in] sheet 6061-T6 aluminum brackets with the rod end sandwiched between them. These brackets are bolted to vertical fiberglass panels that are glued to the chassis. These upper a-arm brackets load the vertical panels in the plane of the panels.

The front suspension uses Army/Navy or military spec nuts, bolts and washers. All structural brackets are secured to the chassis with at least 3 bolts.

2.2 Wheels and Tires

Centaurus I will be using NGM wheels with Bridgestone Ecopia tires in all races. The left side hub uses a LH threaded nut, and the right side hub uses a RH threaded nut to insure retention. Also all hub nuts utilize safety wire to prevent loosening.

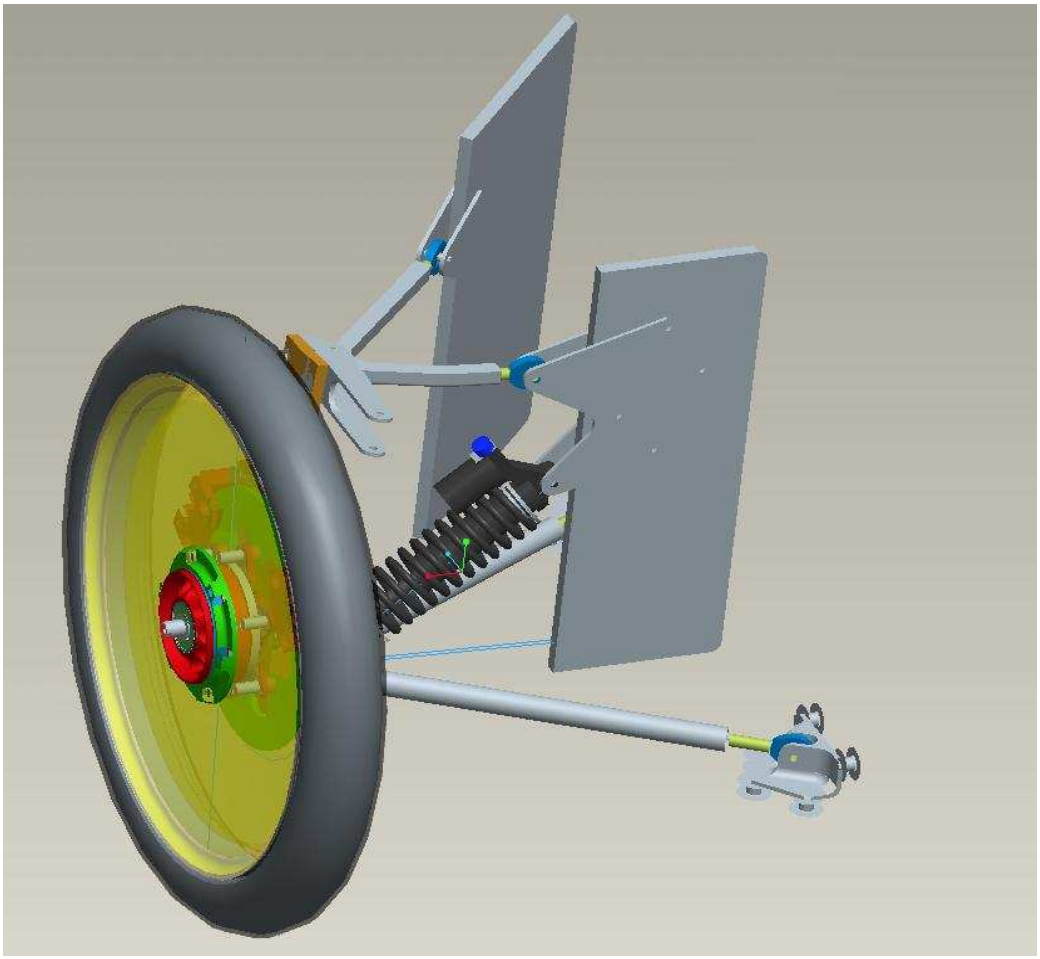

2.3 Front Suspension Stress Analysis

First free body diagrams were constructed for the upright and a-arms. Using the fact that the sum of moments and the sum of forces equals 0 the reaction forces in all members were solved for. The input forces for these equations are the vertical force on the tire (Wr) the braking force (Fb), and the cornering force (Fc). For the worst case scenario loading (1 [G] right turn, 1 [G] braking and a 4 [G] bump) the highest force in the lower A-arm is 1517 [lbs] and the highest force in the upper A-arm is 427 [lbs].

The bending moments in the upright were calculated using previously calculated reaction forces. The maximum stress was found at three critical cross sections and this resulted in a safety factor of 5.59 for yielding and 1.76 for fatigue strength for 7075-T6 Aluminum.

Finally a buckling analysis was performed on both upper and lower a-arms. The Euler mode of buckling was found to be applicable for the lower a_arm and the upper a_arm both Johnson and Euler buckling modes were analyzed. The result was that the lower a-arm has a safety factor of 21.96 with respect to failure in buckling, and the upper a_arm has a safety factor of 8.82 with respect to buckling.

Free body diagrams and values for reaction forces can be found in the appendix, section one.

3 - Rear Suspension

3.1 - Rear Suspension Stress Analysis

Assumptions

The calculated forces acting on the rear suspension utilized the assumed static load of 200 [lbs] on the rear wheel, with 1G cornering forces equaling 200 [lbs], and 4G bump loads equaling 800 [lbs]. Forces due to braking and acceleration were ignored due to their relatively small magnitude..

Reaction Forces

The first step in determining the forces in the system was to determine the reactions at chassis mounting points. The following figure demonstrates all the forces acting on the system. In this case, the car is turning right.

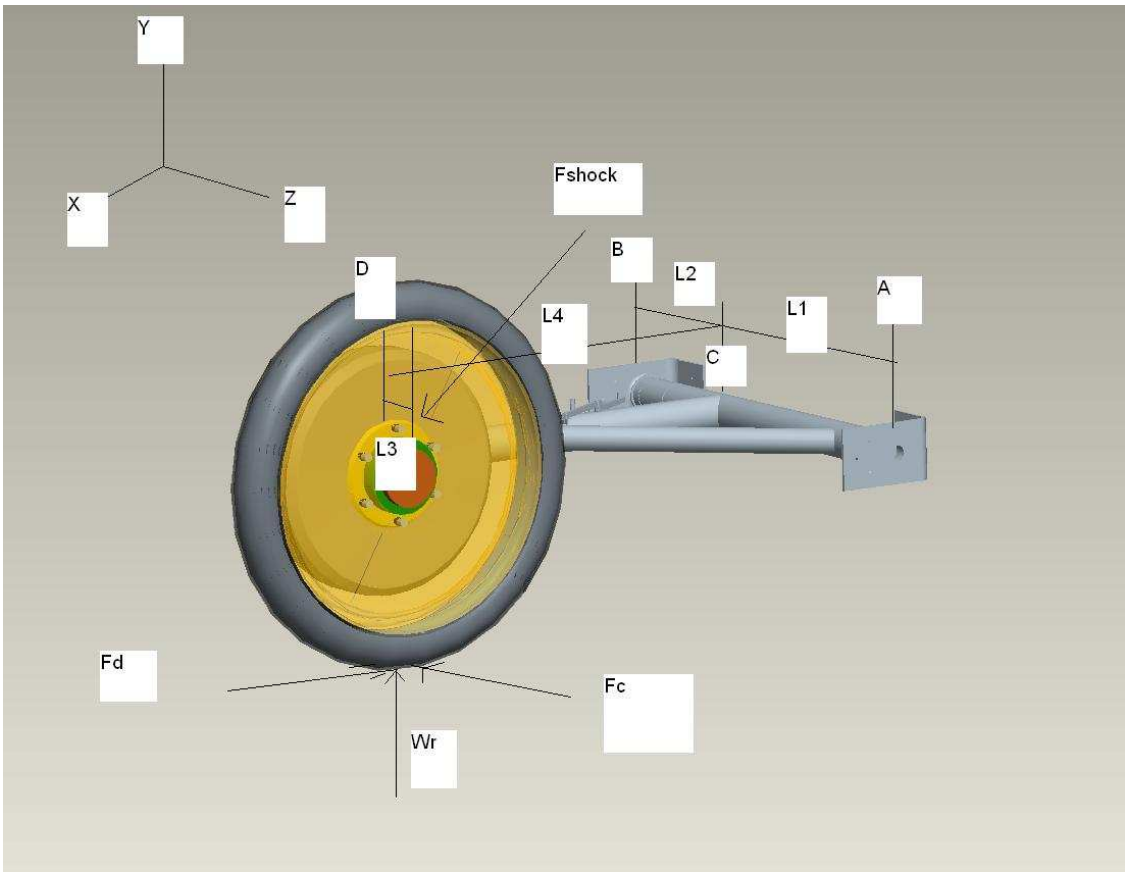

Coordinates (in inches)			
Point	**X**	**Y**	**Z**
A	0	0	21
B	0	0	0
D	21.625	0	7.125

Statics equations were developed to trace cornering forces (Fc) and weight back to points A, B, and C (shock mount point). Then a spreadsheet was developed to allow for different dimensions, weights, bump, and cornering forces. Six different loading combinations of Fc and Wr were examined as shown in the Appendix. The largest force at point B occurs in a 4 [G] bump and 1 [G] left turn. During these conditions, the bracket at B is subjected to 907 [lbs] in the -x direction, and 67 [lbs] in the y direction. The largest force at point A occurs

during this situation as well, with 503 [lbs] in the negative x direction and 67 [lbs] in the negative y direction. Loads in the z directions are only felt at point A by design where a snap ring holds the bearing in place. At point B the bearing is allowed to slide in the z direction so that no additional stresses are put on the chassis by holding the swing arm. The table of calculated reaction forces is found in the appendix, section two.

Stress analysis was performed for components of the rear suspension which
are made of the following materials.

Material Property Information:
7075-T6 Aluminum
Yield Strength Sy= 73000 [psi]
Normalized 4130 Steel
Yield Strength Sy= 75000 [psi]

3.2 Swing Arm Mounting Brackets

The swing arm is attached through brackets machined out of 7075 aluminum located at points A and B. Each bracket contains bearings and is attached to the chassis using five grommets. Each grommet can handle 1500 [lbs] of shear load, so that the combined grommets of each bracket can easily the maximum loads at A and B as stated above.

3.3 Swing Arm

The swing arm experiences the greatest stress nine inches forward from the axle, where the cross support tube attaches to the swing arm. Under the 4[G] bump and 1[G] cornering case, tensile, bending, and torsional stresses exist on a plane.. Each stress component was calculated, and then the equivalent principal stress at this point was determined and compared to the yield strength of 4130 steel in a safety factor calculation.

The tubing of the swing arm has the following geometric properties:
Cross-sectional area [in^2]= .3440
Cross-sectional moment of inertia [in^4]= .1223
Polar moment of Inertia [in^4]= .2446
Outer diameter [in]: 1.75
Wall thickness [in]= .065

The resulting stresses on the plane are:

Torsion:	4704.48 [in-lbf]
Torsional Stress:	16,829.49 [psi]
Bending Stress:	11,590.35 [psi]
Principal Stress:	25,384.5 [psi]
Safety Factor:	2.95

3.4 Parking Brake

The parking brake acts at the rear tire. Calculations were done to ensure that if the rear tire is locked in place, the car will not slide down a 10% grade. The parking brake utilizes a four bar over-center linkage, which allows for locking of the brake, and provides a mechanical advantage. Experimentation will be done in order to determine the range of motion necessary to lock the tire, and car in place. Safety factor calculations will be done when the design is fully complete, in order to make sure that the design will not fail.

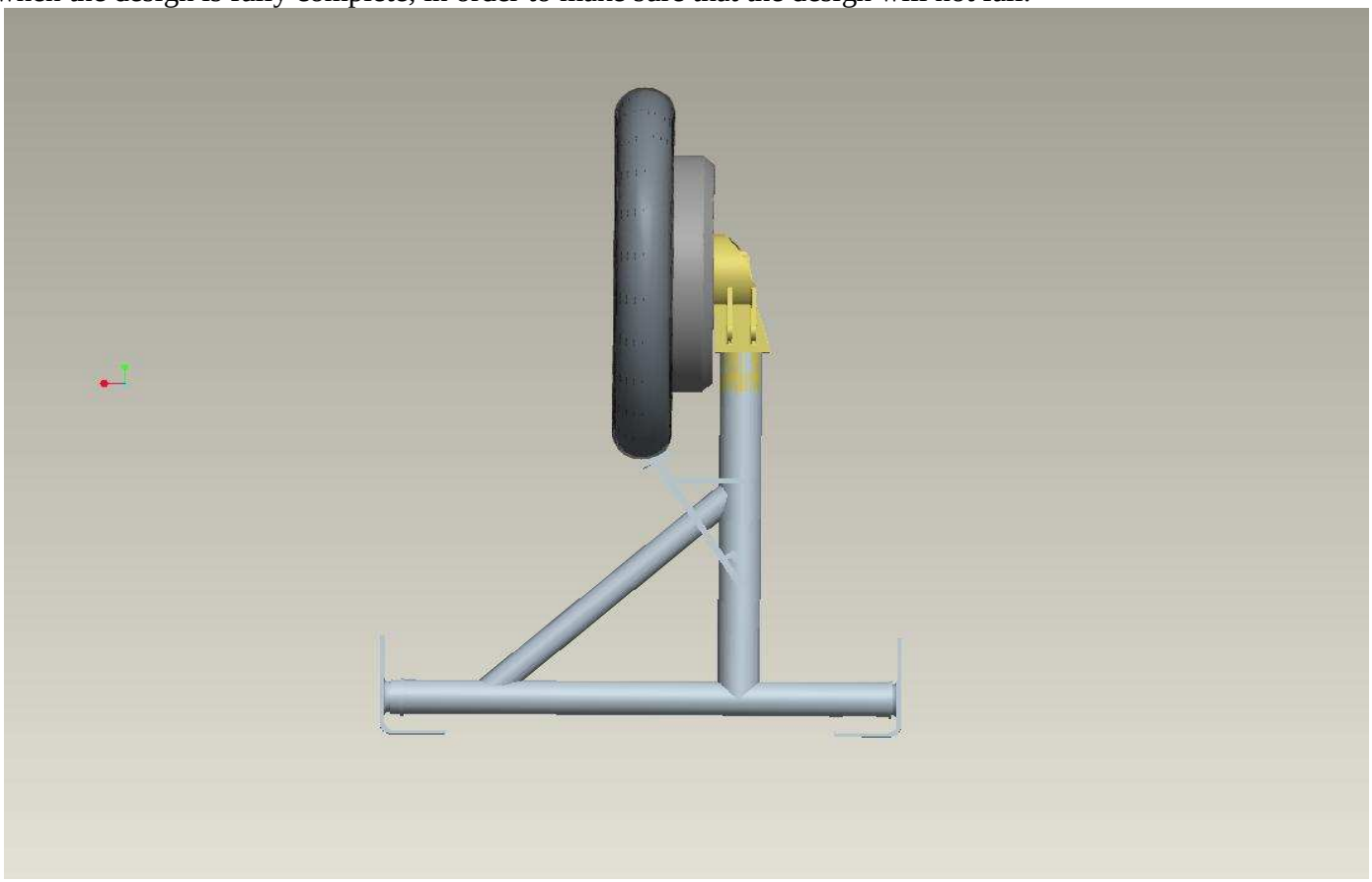

The above drawing shows the parking brake as mounted on the swing arm. A push pull cable actuates the design, and is connected to a lever for the driver to use.

4 - Chassis

4.1 - Introduction

To achieve the best design the car was built with a lightweight monocoque frame. The predicted total weight of the vehicle including driver and batteries is 600 [lbs]**.** The composite frame accounts for 45 pounds of the total vehicle weight. By placing the batteries in the front of the vehicle the driver is allowed more crush space, while maintaining a center of gravity behind the front axle line.

The chassis includes a composite frame integrated with the bottom of the vehicle's shell, suspension components, and roll cage. The chassis is designed to transfer loads from the driver and other components to the suspension mounts. The top shell is completely detachable from the chassis to allow redirection of the array while the car is stationary. The shell also has a removable canopy for driver egress.

The driver seated in the cockpit is fully enclosed and isolated from the road and is clear of all moving parts. The cockpit contains a six-point harness, headrest, and a driver ventilation system. The cockpit is designed to me requirements for driver visibility, vehicle impact protection, and provide unstressed driving of the vehicle.

4.2 - Mounting to Composite Paneling

Two part 5319 SERA aluminum inserts (grommets) are used at all locations that require fastening to the composite panels. The aluminum inserts are tested by the manufacturer to 1500 [lbf] for in-plane shear and are used for all attached components under load. The design of the insert is intended to handle bolt clamping load while distributing axial and shear loads to the sandwich panels. These inserts were used successfully on all previous U of M solar vehicles.

4.3 - Chassis Construction

Monocoque refers to the construction method that directs the forces in the chassis through the skin of the composite material. The fiberglass paneling we have chosen offers several advantages over a space-frame chassis. Fiberglass paneling offers the same lightweight and high strength advantages as an aluminum space-frame design, while providing a fully enclosed space for the driver, attachment points for electrical and suspension components, and significantly simplifying construction and design over a space frame.

Fiberglass paneling owes its great strength to the interlacing fibers in the skins of the paneling. The facing acts like thousands of tiny cables all strung in the same direction held in place by the matrix of resin combined with the facing fabric in its production. Many fabrics are available, examples being Kevlar, glass, carbon, and fiberglass. Each has a specific property that is advantageous. Fiberglass paneling was chosen for out chassis because of its high strength to weight ratio, non-conductive electrical properties, and energy dissipation during impact failure.

The paneling is constructed in a box-beam geometry with panels assembled perpendicular to each other. The panels also have interlocking tabs and slots at all joints for improved strength, simplified assembly, and consistent high quality joints. The panels were designed in such a way that all loads are transferred into the chassis in a direction parallel to at least one prefabricated panel.

A mock-up full-scale plywood chassis was constructed before the chassis design was finalized to have a model of the driver cockpit. It helped to integrate the roll bar, pedals, steering, and driver visibility. A complete vehicle assembly in Pro Engineer was also used to enhance the integration between all vehicle parts. The combination of these two tools assisted driver placement, layout of components, and integration of vehicle systems.

4.4 - Material Specifications

Hexcel Fibrelam grade 5 prefabricated fiberglass paneling was used to construct the chassis. The panels have a thickness of 0.400 [in] consisting of Nomex honeycomb core, cell diameter 1/8 [in], and a nominal thickness of 0.380 [in]. Each side of the core is covered with fiberglass fabric. The paneling has an average weight of 0.52 [lbs/ft^2]. Data from the published four point bending test was used to show maximum allowable stress in the face sheet of 61,400 [psi]. See appendix for stress calculations.

3M^{TM} Scotch-Weld^{TM} DP-460 NS was used to join the paneling at all joints. This glue is very similar to glue used on previous cars but has a much higher viscosity which assures us that it will not flow away from the joints and will maintain correctly shaped fillets. The epoxy is rated at 4900 [psi] under the surface preparation conditions used and room temperature curing. The typical joints on the car have approximately 0.400 [in^2] of shear area per joint inch. See figure 4.1 below. The joint can then be assumed to carry a maximum shear load of (0.4 inches)(4900 psi) = 1960 [lbf] per inch of joint.

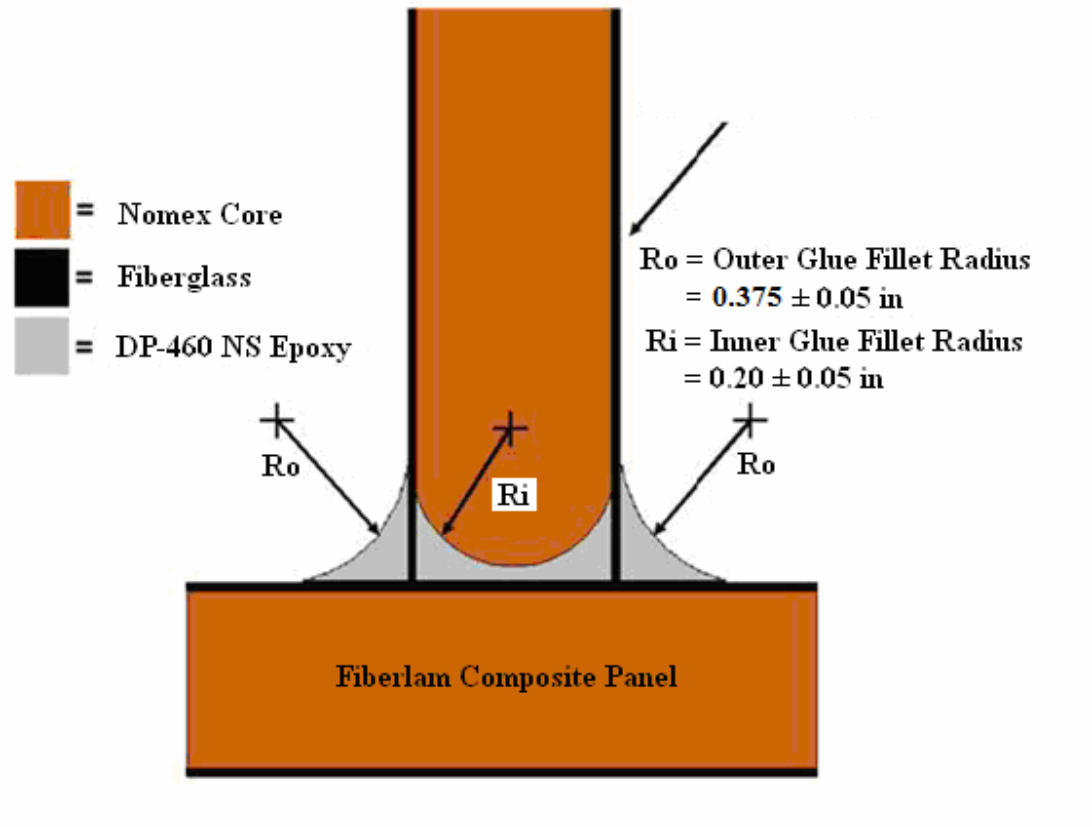

Figure 4.1: Chassis Joint Bond

4.5 - Construction

The process used to machine the 4.0 [ft] by 12.0 [ft] panels was water jet (abrasive) cutting. This process uses a high-pressure stream of water combined with a garnet aggregate to erode away the material it cuts. The mixture of water and garnet is pressurized to 40,000 [psi] and focused through a carbide tip into a beam that is 0.042 [in] in diameter. The water jet tool is the best suited tool for cutting this type of fiberglass paneling because there is no clamping needed, no fibers are released into the air, no forces exerted on the material by the tooling, and it cuts to very high tolerances.

The paneling was placed on a bed of plastic/cardboard energy absorbing material, which is above a steel water tank. The paneling was held in place by its own weight, no clamping was necessary. After the paneling was cut

it was quickly cleaned off and dried. The paneling was also laid out in a warm dry environment for two days to ensure all the moisture was removed from the paneling before it was glued together.

The paneling was prepped by abrading all glue surfaces followed by extensive cleaning of the glue joints with isopropyl alcohol. Using 3M™ Scotch-Weld™ DP-460 NS two-part epoxy the composite paneling was assembled. The epoxy was applied using the 400 [ml] Pneumatic Thunder Epoxy dispenser adapted with 10 [mm] deluxe mixing tips to ensure complete mixing between the resin and the hardener. The epoxy was filleted with a 0.250 [in] radius on the joints, which adequately transfers the forces from one panel to the next as if the chassis was a unified piece. Many of the chassis joints are also reinforced by the attachment brackets of the roll bar, suspension, and other components on the car.

4.6 - Crush Space

In the event of a collision, a system of progressive safety features will prevent the driver from being injured. The design places the driver within a safety capsule, with no part of his or her body extending beyond the structural chassis. The driver's head will be encompassed by a roll cage structure designed to protect the vulnerable driver's head which protrudes through the car's body.

NASC rules require 15 [cm] of horizontal distance between the driver's shoulders, hips and feet and the car's outer body surface. Centaurus' minimum crush space of 17 [in] is almost three times that required by ASC rules. This large crush space around the driver was made possible by locating the cockpit in a central location in the car. In a rear collision, the 122 [in] of solar car behind the driver will act to absorb much of the impact energy. Likewise, in side collisions the driver resides in the center 22.0 [in] of the 70.5 [in] wide car, allowing over 24 [in] of crush zone on either side. The shell material will crush and the driver is then protected by the driver's compartment as shown in the various crash analysis sections which follow.

Front crush space was maximized beyond race rule requirements with 17 [in] of crush space. The nose of the car will crush easily, allowing the crash to be stopped by the structural chassis. The front batteries will help block penetrating objects and decelerate the impacting body due to their mass.

Driver Restraint Description

4.7 - Driver's Compartment

The driver's safety capsule is designed to remain un-violated in the event of a collision and constrain the driver inside. The 22.0 [in] driver's compartment width holds most drivers snug from left to right which would be beneficial in a side impact. Also, the drivers lower extremities are confined within the driver's compartment from all sides and cannot "flail" in an accident. The side panels are 14.0 [in] high, and when belted in, only the upper portion of the driver is above the upper plane of the chassis. The driver head is constrained from moving rearward during a rear impact by the seatback and a padded headrest. This reduces the risk of a whiplash injury. See figure 4.2 below for a view of driver positioning (note, the head rest and back panel have been removed for clearer viewing of the rollbar).

4.8 - Safety Harness

A six-point safety harness will be utilized. The rear harness attachment points are combined with the seatback and rollbar cross-brace (see figure 4.2), providing strength in multiple directions. The front harness attachment is at the lower intersection of two chassis body panels and the rollbar brackets. The driver is reclined at approximately 27 degrees from the vertical. This rule provided a guideline for harness mounting point locations. The shoulder belts are secured slightly above the shoulder to prevent injury incase of a head-on collision, and also constraining the driver in the event of a roll over. The lap belts are positioned 3 inches ahead of the intersection of the belly pan and seat back. This ensures that the belts cross the hips and not the lower abdominal region. The submarine belts secure to the same location holding the driver in a frontal collision.

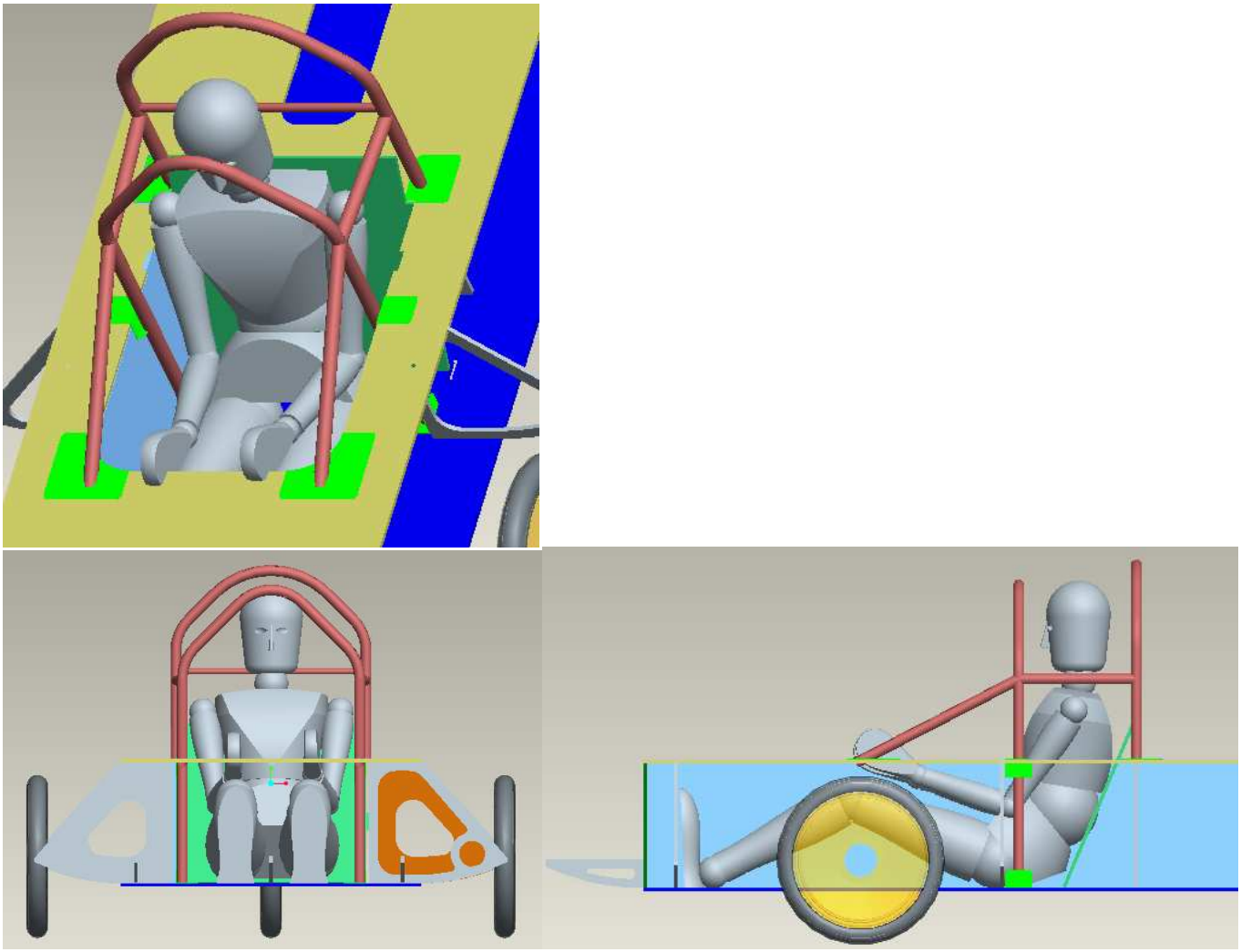

Figure 4.2: Driver Location in Compartment

4.9 - Roll Cage

The roll cage is comprised of four components:

- A hoop in front of the driver, with legs that extend down to the bottom of the chassis. It is attached to the chassis at the bottom edge of the driver compartment (floor of the chassis) and the side panels via inserts, along with flanges on the top of the chassis via inserts.
- A rear hoop behind the driver welded to flanges and attached to the top of the chassis via inserts. The seat back is also placed inside the hoop and constructed from the same fiberglass panels as the main chassis, to add structural rigidity in case of impact.
- Two supports welded between the front and rear hoops to improve front-to-back support and reduce the chances of either hoop buckling.
- Two forward facing supports welded to the front hoop and attached to the chassis's top panel via inserts. These supports are installed to deflect any oncoming panels over the driver's head in a frontal collision, as well as improve front-to-back strength.

The entire structure is constructed from 1.250 [in] outside diameter 4130 steel tubing with a 0.049 [in] wall thickness and from 0.065 [in] 4130 sheet steel for the brackets mounting the rollbar to the chassis. The tubing is cold drawn normalized with yield strength reported as 75,000 [psi]. This tubing has an EI (Young's modulus multiplied by moment of inertia) stiffness that is 27.5 % larger than the 2.5 [cm] OD by 2 [mm] wall tubing as

specified in the NASC rules. The larger EI stiffness improves the overall strength, critical buckling load, and crumpling resistance. All welding was professionally done using the TIG welding process.

Crash Loading Analysis

4.10 - Total Mass and Center of Gravity

Coordinate	Reference		Wt Distribution	
X	Centerline		Front	Rear
Y	Ground		66.5%	33.5%
Z	Front Axle			
Component	**Mass (lbm)**	**X (in)**	**Y (in)**	**Z (in)**
Chassis Panels	44.6	0.0	13.6	-29.2
Shell	97.0	0.0	18.1	-52.9
Batteries	70.0	-3.0	9.4	29.5
FS	30.0	0.0	8.9	0.0
RS	70.0	1.8	9.5	-85.5
Steering	3.0	0.0	17.3	1.6
Brakes	4.1	5.0	24.4	23.1
Rollbar	13.7	0.0	26.0	-19.0
Driver	170.0	0.0	12.4	-15.7
EE box	20.0	0.0	13.9	-55.0
Array	46.4	0	25.2	-62.1
Total	**568.8**	**-0.1**	**14.1**	**-30.2**

4.11 - Front Collision

The loading on various panels will be traced and specific joints and panels will be analyzed for strength using accepted procedures based upon the properties of the panels and the bonding agent.

The bumper height ranges from 13.8 [in] to 17.7 [in] and the front chassis lateral bulkhead ranges from 6 [in] to 20 [in]. Thus the bumper will hit the chassis bulkhead and battery box, once the nose collapses. The body may or may not move rearward as the nose collapses. If the latch and guides for the body fail and the body moves rearward, the driver canopy will hit the front roll hoop and the supports and deflect up and rearward, coming off of the car. The canopy opening extends forward on the body approximately 24 [in] ahead of the driver's head. If the body moves rearward, the edges of the canopy opening will hit the forward roll bar hoop which will either deflect the upper body above the driver, or start tearing the body apart. Eventually, the bumper will contact the battery box and the front chassis bulkhead.

Each of these component weights is multiplied by five to estimate the 5 [G] loading. The center of mass of the front battery pack is within the bumper height, and the battery pack is in front of the front bulkhead, so the inertia force due to the front battery pack acts directly upon the bumper. It does not load the chassis in a front end collision. Thus the load on the chassis can be reduced by the 5 [G] force on the battery pack i.e. Force from bumper upon chassis = 5 * (570 – 70) = 5 * (500) = 2500 [lbs]. This load will be initially felt by the two vertical panels, one on each side of the driver. The front chassis bulkhead is glued to these panels, and so will distribute the bumper load across the front vertical face of each panel.

The following will argue that the forces are taken by these vertical panels and have sufficient strength to withstand front bumper loads under very conservative assumptions. The upper and lower panels are used to provide edge stability to the vertical panels and are not figured into the crash analysis. The inertia forces on the driver, body, and chassis will all be assumed to be located at the rear of the driver's compartment, and will only be resisted longitudinally by the two vertical panels. These panels are a minimum of 14 [in] high and 90 [in]

long. This is a conservative estimate because some of the impact forces would be transmitted to the upper and lower panels as well as the vertical panels. Each panel has similar loading, so only one will be examined. The presumed mode of failure is buckling, and the critical stress level can be found using the methods in Successful Composite Techniques, by K. Noakes, Osprey Publishing, 1992, p 133 – 141. The critical buckling force is given as:

$$f_b = \left(\frac{d}{b}\right)^2 EK$$

where d is the distance between outer fiberglass skin median planes, b is the width of the panel, E is the modulus of elasticity for the skin, and K is an empirical buckling stress coefficient related to core material and panel geometry. Inputting the appropriate values into the above equation, the critical buckling load is:

$$f_b = \left(\frac{0.395}{14}\right)^2 (9.13E6) * (1.2) = 8723lbs$$

As such, the panels will not fail due to buckling, since the load induced from a 5G impact is roughly ¼ of the buckling load. Therefore, failure of the panels will be based on the ultimate stress for compression. The cross-sectional area of the fiberglass skin of the vertical panels is
$A = 14*4*0.010 = 0.56\ in^2$. Applying the 5G load gives a stress of $\sigma = 2500 / 0.56 = 4464$ psi, which is less than the maximum allowable skin stress of 61,400 psi by a safety factor of 14. Thus, the chassis and driver's compartment can easily withstand the 5G impact.

4.12 - Rear Impact

The trailing edge of the vehicle at nominal ride height is 14.1 [in], while the bumper ranges from 13.8 [in] to 17.7 [in]. Upon impact, the bumper will strike the tail section of the body which will start to collapse and be driven forward. The roll bar has a rear hoop and seat panel which will prevent the body from impacting the driver. The bumper will then strike the rear wheel. The combined mass of the motor, rear wheel, and rear suspension is 70 [lbm], which will absorb some of the impact energy and slow down the impacting vehicle. Finally the bumper will contact the rear chassis bulkhead the same was as for the front impact. The bulkhead will distribute the load to the two longitudinal vertical panels. It has already been shown that these vertical panels can easily handle this 5 [G] impact. The only difference here is the added front battery pack inertial loading. This creates an inertial loading of approximately 570 [lbf] and a compressive stress of 5089 psi, which yields a safety factor of more than 12 against compressive failure and a safety factor of more than 3 against buckling. Thus the chassis can also withstand a 5G rear impact.

4.13 - Bending Rigidity Under Vertical Load

To assess the side impact and rollover strength of the chassis, it is necessary to estimate the bending moments caused by inertial loads of components and the locations of the chassis supports. The supports are the rear structural chassis plane and the front axle line. If we presume the entire vehicle weight to be concentrated at the CG, this produces a bending moment of $M = R_f * L_{CG} = 324lb*27.3in = 8845$ [lb-in], located 27.3 inches rearward of the front axle line, near the front of the opening in the top panel for the driver compartment. This is also the section of the chassis with the lowest moment of inertia, so if failure were to occur due to bending, it would occur at this location. The moment of inertia of only the fiberglass skin in this section is 51.9 [in^4]. Using the equation for stress in a beam in bending, $\sigma = My/I = 8845lb\text{-}in*9.5in/51.9in^4 = 1620$ [psi]. Comparing this to the maximum skin stress of 61,400 psi, we have a safety factor of 38 with regards failure under static loading. In the event of a large bump, or rollover conditions, where a large vertical load is applied to the chassis, the same approach can be applied. Using a vertical load of 5G, or 2850 [lbs], the safety factor reduces to 7.5, meaning the chassis will not fail in bending under a vertical load.

4.14 - Side Impact at 5G

This will be treated similarly to the front/rear end collisions. The driver is within the center 22.0 [in] of the 35 [in] wide structural chassis, with the forward roll bar hoop ahead of the driver's head, and fore-aft supports on each side cradling the driver's head, and a rear roll hoop behind the driver's head. The side impact will be considered a plane which contacts the vehicle, crushing the over 16 [in] of body and array before impacting the structural chassis. The canopy would contact the rollbar hoops and fly off, and the body which angles upward toward the driver from the side would slide upward along the roll bar hoops and/or tear itself apart on the roll bar and the fore and aft supports. Eventually the side of the chassis would be contacted.

Again we presume that the rearmost chassis panel and front axle line are the supports, and that the 5G impact is applied near the CG and driver compartment opening. The bending moment will be M=5*8845 = 44,225 [lb-in]. In the lateral direction, the cross sectional moment of inertia of the fiberglass skin is I = 193 [in^4]. Using the beam bending equation, the maximum stress is
σ = 44,225lb-in*17.4in/193in^4 = 3987 [psi]. This gives a safety factor of greater than 15 against bending failure from a lateral impact.

4.15 - Rollover Analysis Methods

When the vehicle is in a rollover condition, the roll bar and the front of the chassis will support it. The following will show that the roll bar structure is able to support the majority or all of the 3G load at various angles. These loads will then be transferred to the composite chassis, which it has already been shown is more than capable of handling such loads.

Rollbar simulation was done using finite element analysis (FEA). The software package used was ANSYS Workbench version 11. All simulations were done as static structural using tetrahedral elements and a relevance factor of 60. Because it has been shown that the chassis can support many times the 3G loads being investigated, the attachment points of the rollbar to the chassis were modeled as rigid supports. Loads were applied on a ½ inch by ½ inch square patch added to the rollbar normal to the loading direction to provide a convenient geometric surface. Also, all loads were applied solely to the front hoop. This was done as a "worst case" scenario, since the rear hoop will have additional support from a fiberglass panel inset into it, and thus will be stronger than the front hoop. Also, in a real situation it is likely that both the front and rear hoops will share the loads, as well as the front or rear edges of the chassis, depending on the impact angle. Stresses were calculated using the von-Mises equivalent stress model. Additionally, because rollbar analysis was done prior to design completion of all components of the vehicle, a conservative weight estimate of 650 [lbs], approximately 50 [lbs] larger than the actual vehicle weight, was used in all loading conditions

4.16 - 3G Vertical Load

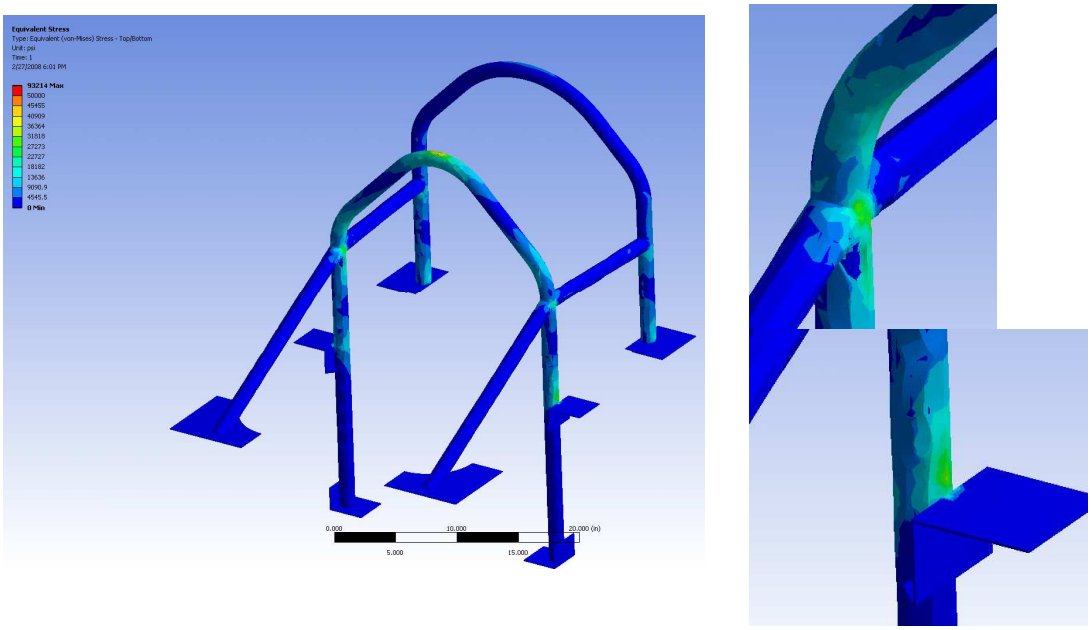

For this load condition, the maximum stresses are seen near the fore-aft supports and where the front hoop passes the top panel of the chassis. The results seem logical, as the bending moments would be highest in the tubing at these locations. The highest stress in these locations is less than 30 ksi, which gives a safety factor of more than 2.5 with respect to the yield strength of the tubing. There were local stress concentrations which peaked above this value, but they were constrained to areas near the small square where the load was applied, and can be attributed to stress concentrations at the corners of this artificial geometry, and therefore have been neglected.

4.17 - 3G Load, 45° Lateral from Vertical

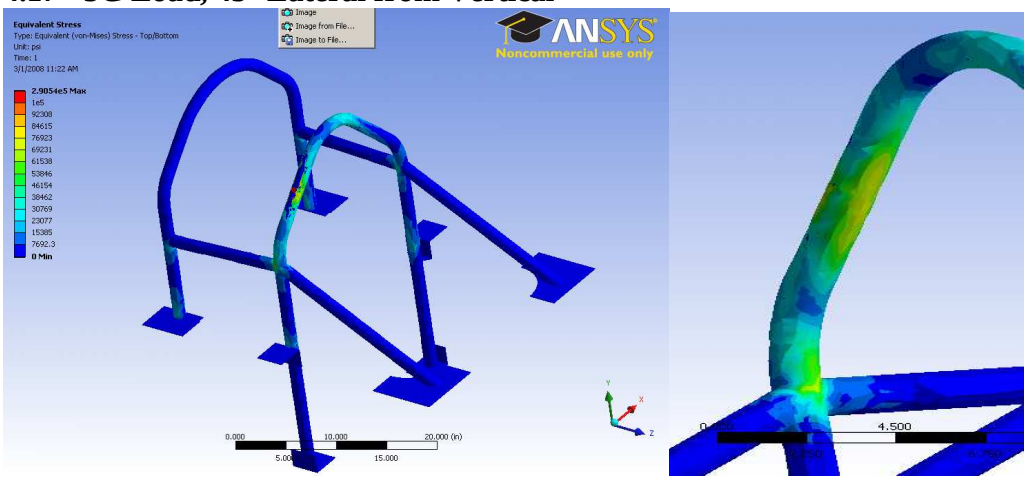

When the load is applied at 45 degrees from vertical the location of the maximum stress shifts to the straight portion of the front hoop. This is because the load was applied at the middle of the straight section, putting it in bending. The peak stresses are near 70 [ksi], which gives a safety factor of 1.1 with respect to yielding. However, again this is a “worst case” scenario, with a single hoop taking the full 3G load. If local yielding were to occur, the other roll hoop or chassis would contribute to the load-bearing. Also, the stresses in the front roll hoop alone, though near yielding, are still well below the failure strength of the material.

4.18 - 3G Load, 22.5° Lateral from Vertical

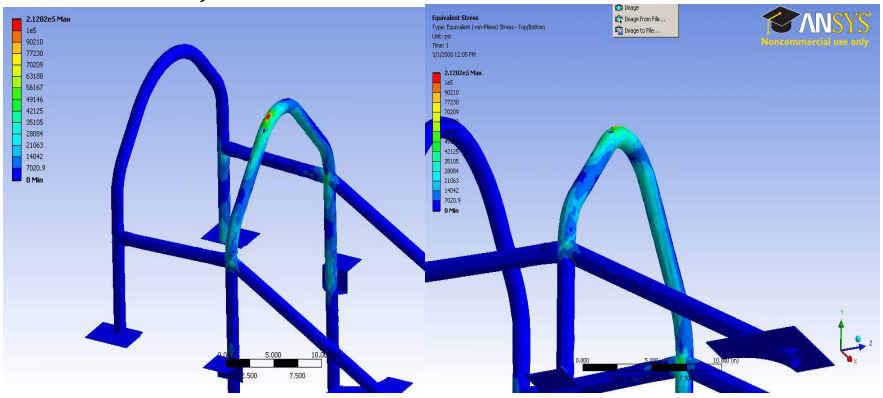

As one would expect, the stresses for a 3G load applied to the front roll hoop 22.5 degrees in the lateral direction from vertical are somewhere between the results for the 45 degree and vertical loads. Because the application point is nearer the peak, the bending stress in the straight sections of the tubing are reduced significantly compared to the 45 degree case, giving a maximum stress of less than 50 [ksi]. This produces a safety factor of greater than 1.5 for this loading condition.

4.19 - 3G Load, 45° Forward from Vertical

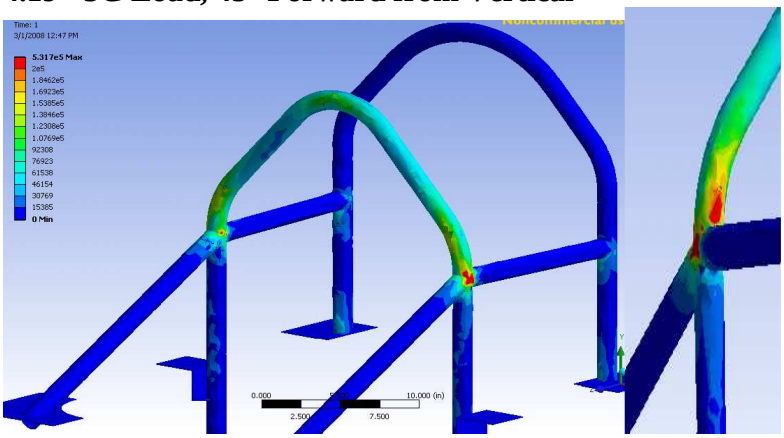

If a 3G impact is loaded 45 degrees from vertical on the peak of the front rollbar hoop, it produces a maximum stress of nearly 150 [ksi]. This exceeds the yield strength of the tubing by a factor of 2. This stress is located just above the intersection of the fore-aft cross braces, where the bending moment is highest due to the rearward component of the impact force. Again, this is a worst-case scenario. In a realistic situation where the force is applied at this orientation, the impacting body or surface that the solar vehicle is impacting against would contact the vehicle in multiple locations. Specifically, at 45 degrees a plane normal to the force would intersect well into the front of the chassis. It can therefore be assumed that in a rollover or other impact with a plane that the front of the chassis would take a large portion of the frontal load and at least some of the vertical load. In this case, the load felt by the rollbar begins to resemble the pure vertical loading condition which can be handled by the front rollbar hoop alone. Regardless, we are investigating either adding supplementary tubes between the front and rear hoops nearer the rollbar peak, or moving the existing fore-aft cross braces higher, to reduce the maximum bending moment in this type of loading, and bring the stresses down to acceptable levels.

4.20 - 3G Load, 22.5° Forward from Vertical

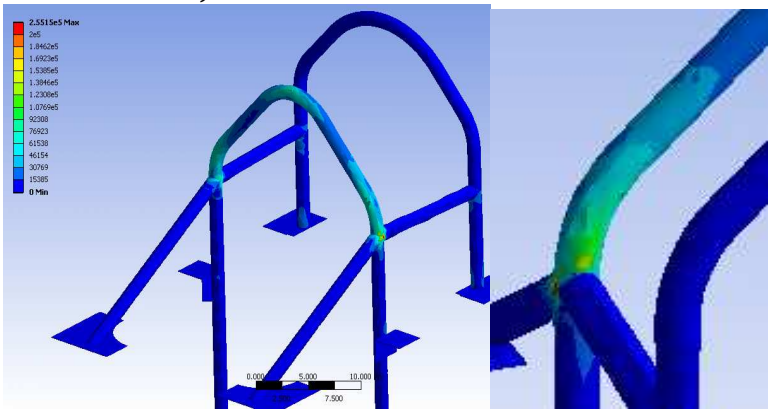

For a 3G impact loaded at the rollbar front hoop peak, 22.5 degrees down from vertical in the frontal direction, as in other loading scenarios a maximum bending moment occurs where the front hoop meets the fore-aft cross braces. At this point, local stresses are seen as high as 100 [ksi], which exceeds the yield stress of the tubing, though it is still lower than the ultimate stress. As was true of the aforementioned loading conditions, this is again a worst-case scenario. The weight of the vehicle has been over-estimated at 650 [lbs], and the full 3G load is applied solely to the front hoop. In this case, the front hoop would yield slightly, dissipating impact energy, and distributing the excess load to other structural members such as the rear rollbar hoop and front of the chassis. However, as was mentioned for the 45 degree forward loading case, we are currently investigating means to reinforce the fore-aft strength the roll hoops, to avoid any yielding of the rollbar for all loading conditions.

4.21 - Battery Enclosure

The Battery box, although not structurally part of the chassis, is made of the same Fiberlam paneling and uses the same non-conductive 3M Scotch-WeldTM DP-460 NS two part epoxy to join paneling. The cells are secured inside the box using a combination of 3MTM Hi-Strength 90 Spray Adhesive and soft foam. This mounting system has been proven on Borealis III and provides a measure of vibration resistance for the fragile electrical connections between cells. The box cover is secured using 4 grommets, the same fasteners that hold on suspension components and will hold the batteries inside the box in the event of a vehicle roll over. The box is removable and is fastened to the chassis by 4 grommets in the same matter. The batteries' weight is distributed to the bottom of the chassis by a set of water jet cut Fibrelam ribs. At least two panels must be penetrated for any of the batteries to contact the driver. Battery cooling is accomplished through the use of two 60mm fans pulling air across a heatsink consisting of copper bus-bar. This air is then vented out of the vehicle through the left wheel well.

5.-Brakes

Centaurus uses two independent hydraulic braking systems acting at the front wheels, assisted by regenerative braking through the motor at the rear wheel.

5.1-Material Specifications

Each hydraulic system has a master cylinder with a 0.75 [in] diameter piston which actuates two cylinders, one at each front wheel. The master cylinders are supplied from CNC Brakes, and are made out of aluminum with steel sleeves. This is a design change from the previous car which used resin master cylinders. The calipers are from Martin Custom Products and have 1.000 [in] diameter pistons. There is a custom 8.000 [in] diameter brake disc at each wheel. The discs are machined from 7075 aluminum and hard coated with "Alpha Coating" from Surface Solutions, Fridley, MN, which provides a surface that is twice the hardness of titanium nitride. A custom pedal assembly actuates both hydraulic systems simultaneously and is adjustable to balance wear on the pads. The regenerative brake is controlled with a lever on the steering wheel. Components were sized based upon an optimistic tire-road coefficient of friction of 1.0, which with front wheel braking only, corresponds to a

deceleration of 0.85 [G] using the design values for wheelbase and CG location. (The value of 1 [G] deceleration shown previously was used for sizing suspension components, but here we need a more realistic value to check pedal force and stresses, and line pressures). A pedal force of 108 [lbf] will supply line pressure of 565 [psi] and produce deceleration of 0.85 [G]. The master cylinders are rated for 1200 [psi]. If one hydraulic system fails the pressure in the remaining system at 0.85 [G] would double to 1130 [psi] which is still below the rated value. The pedal is constructed from 0.5 [in] x 1.25[in], 7075 Aluminum bar stock, machined into a modified I-beam design. The maximum bending stress under a pedal force of 200[lb] results in a safety factor of 4.7. It should be pointed out that the rules require a braking deceleration of 0.5 [G], and at this level, the above pedal force and line pressure will reduce and the pedal safety factor would increase.

Loading Conditions/System Analysis

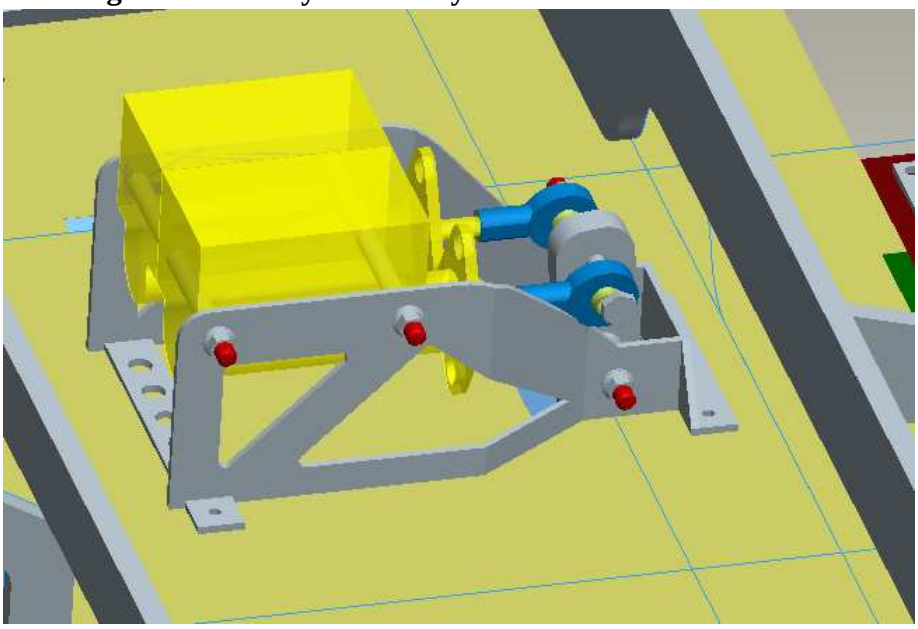

The master cylinder and pedal assembly will be mounted on the top of the chassis with a pedal that drops down into the driver compartment as shown below. The assembly is mounted to the chassis using four grommets capable of withstanding over 6,000[lbs] of shear load. A pedal force of 200[lb] was used in calculating the stresses in the system, which results in a 457[lb] reaction force at each of the master cylinders, and causes internal stresses in the bracket due to the way the master cylinders are attached. This means that only the 200[lb] pedal force will load the grommets in shear. The mounting holes for the bracket were spaced far apart along the front-rear direction in order to reduce the amount of vertical load applied to the grommets. The brackets are waterjet cut from 7075 Aluminum, and bent to the shape shown to the left.

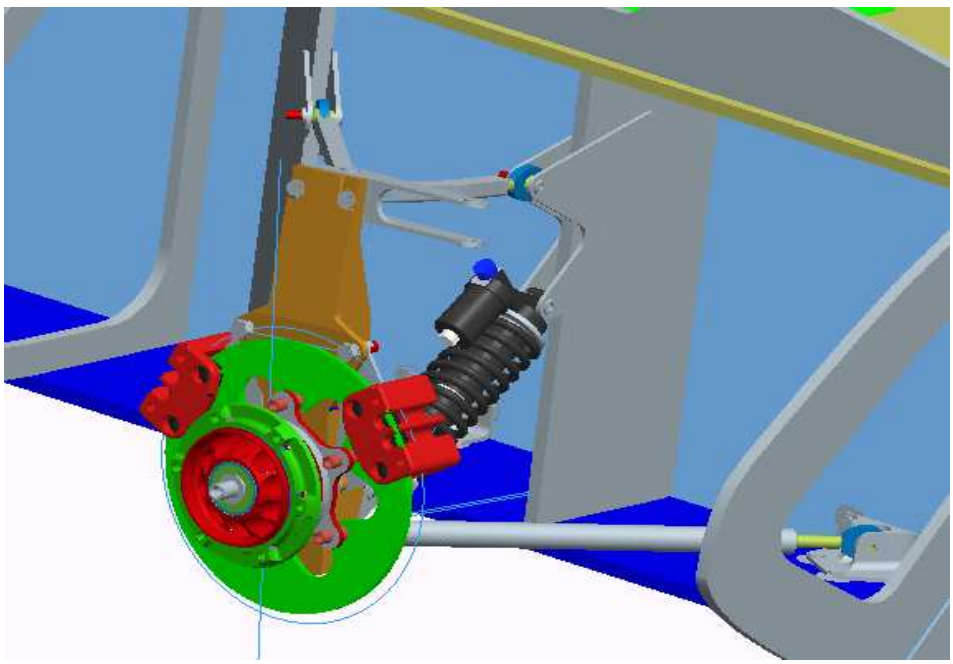

6- Steering

6.1-Material Specifications

Directional control of the solar vehicle is accomplished through the use of a rack and pinion steering system. Driver input and system feedback is relayed througha composite fiberglass and foam steering wheel coupled to a steel steering shaft. A female steel splined insert mates with a steel pinion splined with the corresponding male pattern. The steel pinion gear acts upon an aluminum rack within a custom aluminum housing bolted to the chassis longitudinal panels. Rack motion is transmitted to the front suspension uprights through an aluminum tie rod, steel rod ends, and aluminum steering arms. The circular-shaped rack is preventing from rotating by a piece of Rulon J that acts upon a machined flat portion of the rack and is secured inside the gear box.

Stock components used for the system include: a steel pinion from Stock Drive Products successfully utilized in our previous solar vehicles, a rack machined from a ground 7075 aluminum rod 0.625 inches in diameter, a steering wheel quick release from Mark Williams Enterprises, bronze and Rulon J bushings, and Aurora high precision rod ends. All fastening hardware is aircraft grade AN or NAS series bolts and fasteners. A system overview of the right front wheel is included in figure 6.1.

6.2-Analysis

The steering employs Ackerman geometry as well as minimal bump steer. Steering stability is accomplished by a self-righting moment about the kingpin axis from a 1.14 [in] scrub radius and a 0.831 [in] mechanical trail. The needed steering angle at the wheels was determined from the maneuverability requirements stated in the rules and increased slightly to provide a safety margin.
Loading of the steering system during a 1 [G] corner was used as the worst-case situation for stress on the system. Stress analysis results show safety factors of at least 6.42 on all critical load-bearing components when loaded with 135 [lbf].

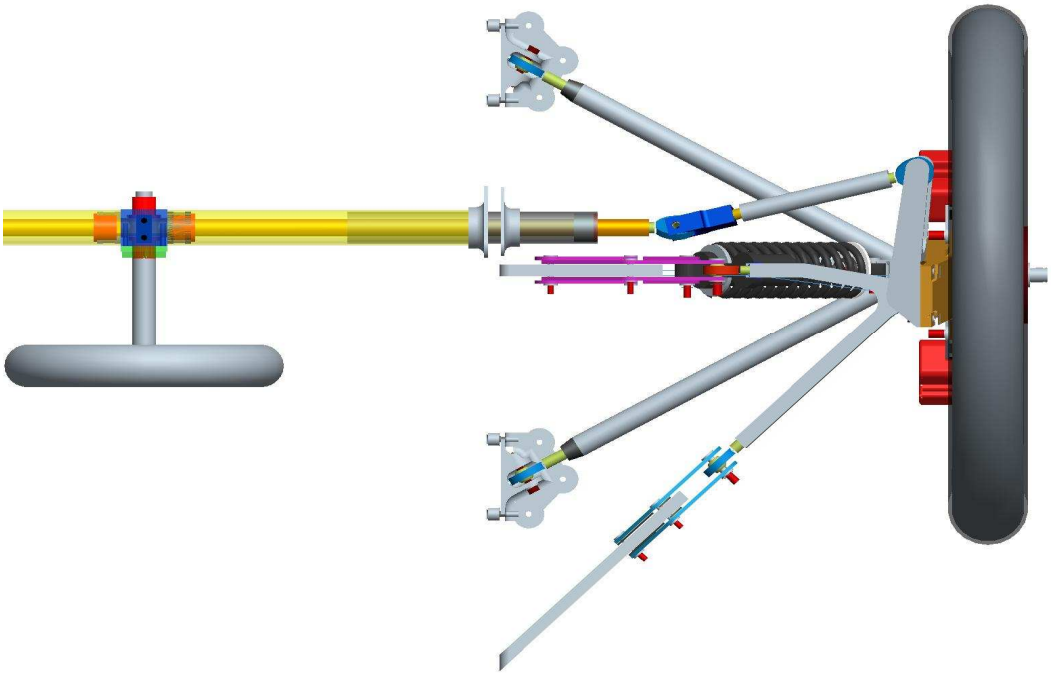

Figure 6-1: Top view of the right front wheel

Appendix

1.- Front Suspension Stress Calculations and Free Body Diagrams
Free body diagram of upright from the FRONT

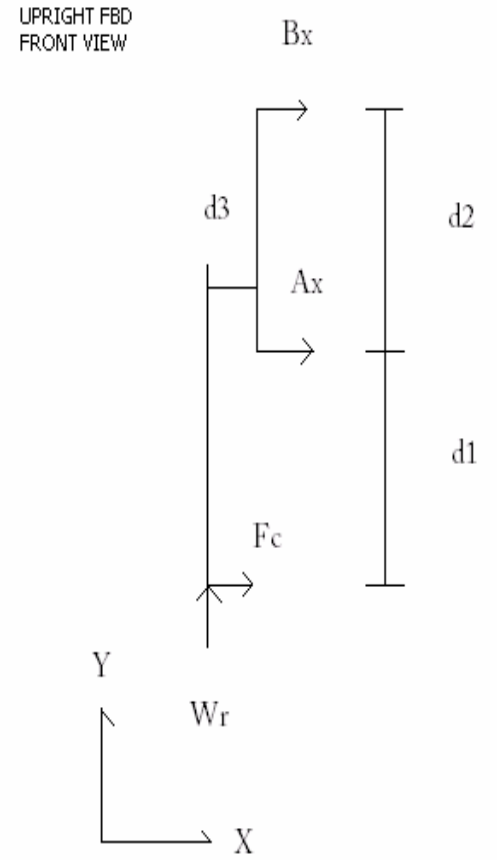

A and B are the upper and lower spherical bearings in the upright. Ax and Bx are reaction forces and d1-d3 are dimensions. Fc and Wr are loads applied to the bottom of the tires.

Free body diagram of the upright from the RIGHT SIDE

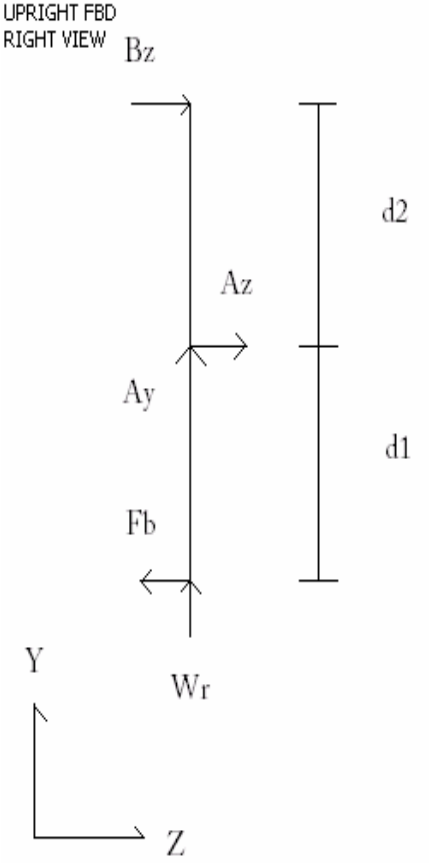

Ay, Az and Bz are reaction forces on the upright and Fb and Wr are forces applied to the bottom of the tire.

Free body diagram of the upright from the TOP

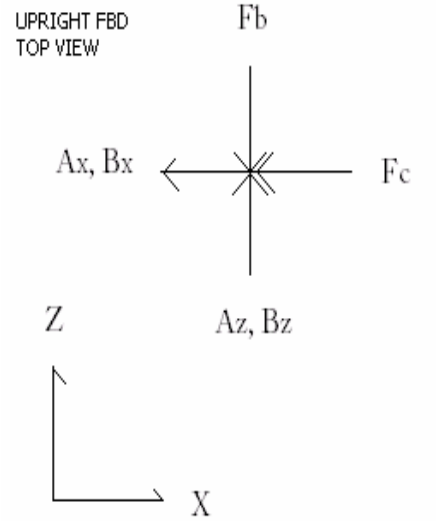

Ax,Bx,Az,Bz are reaction forces on the upright. Fb and Fc are forces applied to the bottom of the tire.

Free body diagram of the lower A-arm from the RIGHT SIDE

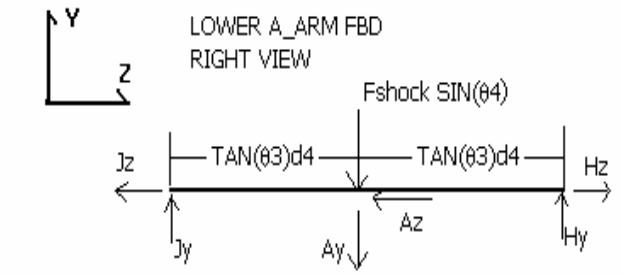

Jz,Jy,Hz,Hy are reaction forces on the chassis. Ay and Az are reaction forces from the upright, Fshock is the force applied by the shock absorber and d4 is a dimension.

Free body diagram of the Lower a_arm from the TOP

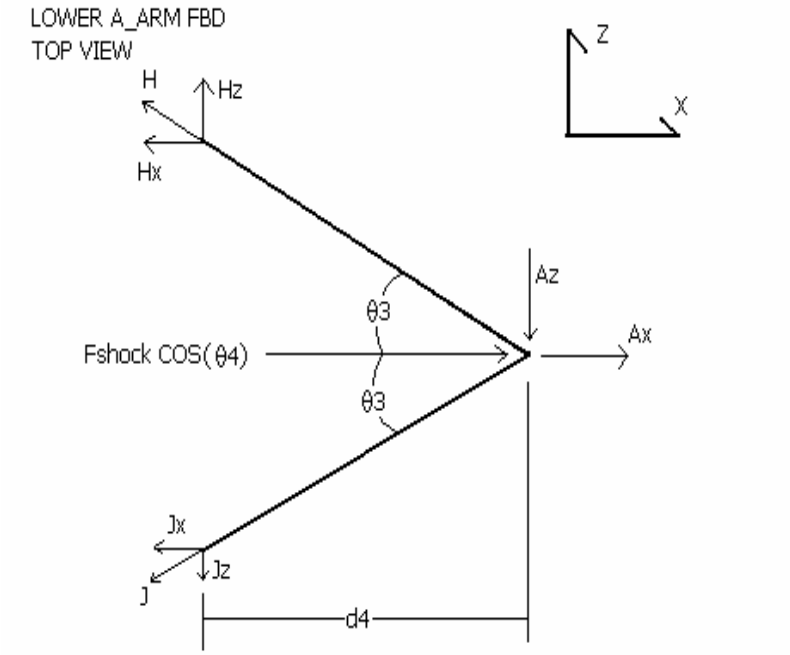

H,Hz,Hx,J,Jx,Jz, are reaction forces on the chassis. Az and Ax are reaction forces from the upright, Fshock is the force applied by the shock absorber and d4 is a dimension.

Free body diagram of the Lower a_arm from the FRONT

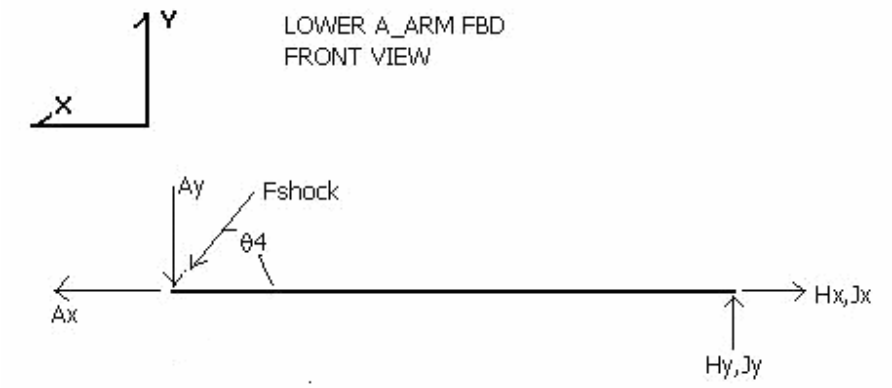

Hx, Jx, Hy,Jy are reaction forces on the chassis, Ax and Ay are reaction forces from the upright. Fshock is the force applied by the shock absorber.

Free body diagram of the upper a_arm form the top

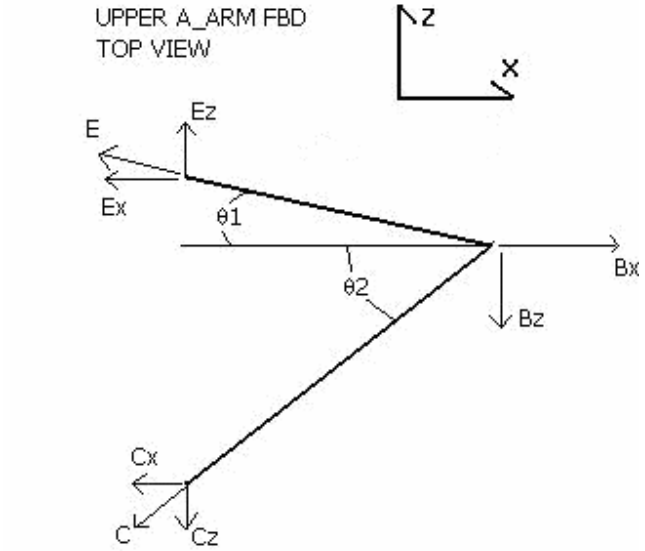

E,Ex,Ez,Cx,C,Cz are reaction forces on the chassis. Bz, Bx are reactions from the upright.

The following is a table of the input forces to the front suspension and the reaction forces at all joints for eight different loading situations. Each loading situation assumes that the static weight supported by each tire is 1/3 the weight of the car or 570/3=190[lbs]. For the situations that include cornering it is assumed that the car is cornering on two wheels therefore 2/3 the weight or 570*2/3=380[lbs] of the car is supported by the outer front wheel and 2/3 the weight of the car 380[lbs] is exerted as a cornering force. All of the situations with braking assume that the weight of the car is distributed evenly between the two front tires 570/2=285 [lbs]. For 4[G] bump situations the static weight supported by the wheel is multiplied by four or 190*4=760[lbs]. All of the loading conditions described in the chart either meet or exceed the loading conditions specified in the structural report instructions.

Known forces	magnitudes(lbs)
weight of car (**W**)	570

Known Lengths	distance (inches)
(d1)	7.6471
(d2)	10
(d3)	1.8
(d4)	13.0337

known angles	
theta1	45
theta2	8.26
theta3	30
theta4	38.7

known angles radians	
theta1	0.785398163
theta2	0.144164196
theta3	0.523598776
theta4	0.675442421

Max Upper A-arm force	427
Max Lower a-arm force	1517

	Situation 1: car stationary	**Situation 2: car traveling straight with a 4g bump**	**Situation 3: 1g right turn no bump**	**Situation 4: 1g right turn, 4 g bump**
Input forces	**magnitudes (lbs)**	**magnitudes (lbs)**	**magnitudes (lbs)**	**magnitudes (lbs)**
Wr	190	760	380	760
Fb	0	0	0	0
Fc	0	0	-380	-380
Output forces	**magnitudes (lbs)**	**magnitudes (lbs)**	**magnitudes (lbs)**	**magnitudes (lbs)**
Ax	34	137	739	807
Ay	-190	-760	-380	-760
Az	0	0	0	0
Bx	-34	-137	-359	-427
Bz	0	0	0	0
C	-30	-121	-317	-377
E	-6	-25	-64	-77
H	157	627	701	1014
Hy	0	0	0	0
J	157	627	701	1014
Jy	0	0	0	0
Fshock	304	1216	608	1216

	Situation 5: 1g braking	**Situation 6: 1g brake 4g bump**	**Situation 7: 1g right turn 1g brake**	**Situation 8: 1g right turn, 4 g bump, 1 g brake**
Input forces	**magnitudes (lbs)**	**magnitudes (lbs)**	**magnitudes (lbs)**	**magnitudes (lbs)**
Wr	285	760	380	760
Fb	285	285	285	285
Fc	0	0	-380	-380
Output forces	**magnitudes (lbs)**	**magnitudes (lbs)**	**magnitudes (lbs)**	**magnitudes (lbs)**
Ax	51	137	739	807
Ay	-285	-760	-380	-760
Az	503	503	503	503
Bx	-51	-137	-359	-427
Bz	-218	-218	-218	-218
C	147	72	-124	-185
E	-278	-294	-334	-346
H	738	1130	1203	1517
Hy	0	0	0	0
J	-268	124	198	511
Jy	0	0	0	0
Fshock	456	1216	608	1216

To determine the stresses in the upright Pro Engineer was used to find the cross sectional area, moments of inertia about both x-x axis and y-y axis, and distance from the centroid in the x direction at 4 different planes. These planes were the plane going through the lower ball joint(A_prime_plane),the plane going through the axle (Axle_plane), and the plane going through the upper ball joint (Upr_BPRIME_plane). Because of the symmetry of the cross section the location of the centroid in the x direction is at the middle.

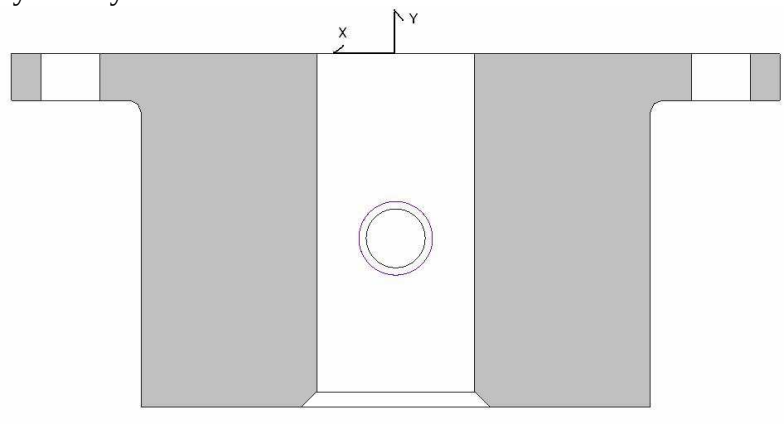

Definitions of Stresses

$$\sigma_X = \frac{M_X Y_X}{I_{XX}}$$

$$\sigma_Y = \frac{M_Y Y_Y}{I_{YY}}$$

$$\sigma_N = \frac{N}{A}$$

$$\tau_X = \frac{V_{XY}}{A}$$

$$\tau_Y = \frac{V_{XZ}}{A}$$

$$\tau_T = \tau_X - \tau_Y$$

$$\sigma_E = \sqrt{\sigma_T^2 + 3\tau_T^2}$$

Safety Factor

$$\mathrm{SF} = \frac{\mathrm{S_y}}{\sigma_\mathrm{E}}$$

To calculate stresses in upright, the worst loading situation was used (4[G] bump, 1[G] turn, [G] cornering) and the bending moment, axial force and shear force were found in XY and YZ plane. The total bending stress was found with the root sum of squares.

Section Properties

cross section location	UPR_BPRIME_PLANE	AXLE_PLANE	A_PRIME_PLANE
cross sectional area (in^2)	0.74779	2.353	0.6645
Ixx (in^4)	0.0107655	0.4657	0.0950195
Iyy(in^4)	0.2298	1.14415	0.4677
y distance to centroid(in)	-0.8409	-0.7153	-0.38

Upright Loading

XY Plane	Bending Moment (lb-in)	Axial(lbs)	Shear(lbs)
UPR_BPRIME_PLANE	0	0	-427
AXLE_PLANE	-3610	760	-807
A_PRIME_PLANE	0	760	807

YZ Plane	Bending Moment (lb-in)	Axial(lbs)	Shear(lbs)
UPR_BPRIME_PLANE	0	0	-218
AXLE_PLANE	-1775.576325	760	503
A_PRIME_PLANE	0	760	503

Upright stresses

UPR_BPRIME_PLANE	calculated stress (psi)
σx	0
σy	0
σn	0
σt	0
τx	-572
τy	-291
τt	-863
σE	1495

AXLE_PLANE	calculated stress (psi)
σx	-12635
σy	-1218
σn	323
σt	13017
τx	-343
τy	214
τt	-557
σE	13053

A_PRIME_PLANE	calculated stress (psi)
σx	0
σx	0
σn	1144
σt	1144
τx	1215
τy	757
τt	458
σE	1392

Safety Factors	σE (psi)	σY (psi)	σY fatigue (psi)	SF actual	SF fatigue
UPR_BPRIME_PLANE	1495	73000	23000	48.84	15.39
AXLE_PLANE	13053	73000	23000	5.59	1.76
A_PRIME_PLANE	1392	73000	23000	52.44	16.52

A arm buckling analysis

Upper A Arm

	Length (in)	Area (in^2)	Ix (in^4)	E (psi)	Sy (psi)	r	L/r	Pcr (lbs)	Buckling	Max_load (lbs)	Safety factor
Arm 1	2.42496	0.197559	0.005099	10400000	73000	0.1597	31.177	11931.88	Johnson	346	34.51
Arm 2	4.97902	0.197559	0.005099	10400000	73000	0.1597	46.49	9384.28	Euler	427	21.96

Lower A Arm

	Length (in)	Area (in^2)	Ix (in^4)	E (psi)	Sy (psi)	r	L/r	Pcr (lbs)	Buckling	Max_load (lbs)	Safety factor
Arm 1	12.9062	0.1261	0.007606	29700000	161000	0.2456	52.552	13384	Euler	1517	8.82
Arm 2	12.9062	0.1261	0.007606	29700000	161000	0.2456	52.552	13384	Euler	1517	8.82

Material properties from matweb.com

2.- Reaction Forces for Various Loading Situations, Rear Suspension

	Input Forces		Output Forces					
	Wr	Fc	Ax	Bx	Ay	By	Fshock	Az
1	200	0	-74.35	-175.46	-39.29	39.29	320	0
2	800	0	-297.38	-701.82	-157.14	157.14	1280.01	0
3	200	200	-280.3	-381.41	51.19	-51.19	320	-200
4	200	-200	131.61	30.5	-129.76	129.76	320	200
5	800	200	-503.34	-907.78	-66.67	66.67	1280.01	-200
6	800	200	-91.43	-495.87	-247.62	247.62	1280.01	200

Case 1 is for when the car is stationary
Case 2 is car traveling straight ahead
Case 3 is 1G left turn, no bump
Case 4 is 1G right turn, no bump
Case 5 is 1G left turn, 4G bump
Case 6 is 1G right turn, 4G bump

3.-Material properties of Fibrelam grade 5 fiberglass paneling

Equations have been obtained from Hexcel Fibrelam mechanical testing data sheets.

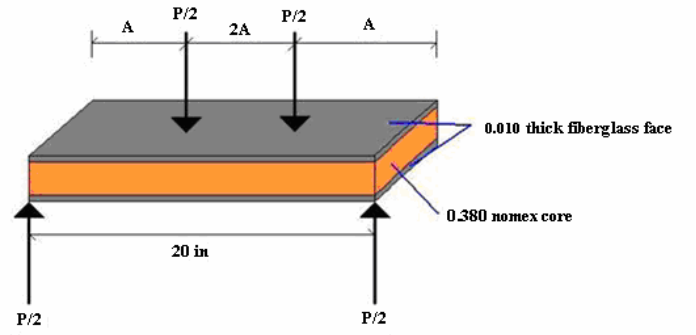

Figure7-3: Four point bending test diagram and data

Variables:

Load at Failure:	P_{crit} = 280 lbs
Deflection Load	P = 100 lbs
Span:	S = 20 in
Distance Between Loads	A = 5 in
Panel Width	w = 3 in
Skin Thickness	t = 0.010 in
Deflection at Middle	d = 0.55 in
Panel Thickness	h = 0.40 in

Critical stress:

Maximum moment is constant and equals

$M_{max} = (P_{crit} / 2)*A = (280 / 2)*5 = 700$ in-lbs

$I_x = I_{0.4} - I_{0.380} = .00228$ in^4

$\sigma_{crit} = - M_{max}*y / I_x = 700 * .2 / .00228$

$\sigma_{crit} = 61{,}403$ psi

61,400 psi will be used in the computations.

Elastic Modulus:

$E = (11/384)*(P/d)*(S^3/(w*t*(h-t)^2)) = (11/384)*(100/0.55)*(20^3/(3*0.010*(0.40-0.01)^2))$

= 9.13E6 psi